Electronic Supplementary Material (ESI) for ChemComm.

# Electronic supplementary material

## Facile electrochemical synthesis of ultrathin iron oxyhydroxide nanosheets for oxygen evolution reaction

Jinshuo Zou, [a] Germanas Peleckis,[b] Chong-Yong Lee,*[a] and Gordon G. Wallace, [a]

[a]ARC Centre of Excellence for Electromaterials Science, Intelligent Polymer Research Institute, AIIM, Innovation Campus, University of Wollongong, Wollongong, NSW 2500, Australia.

[b]Institute for Superconducting and Electronic Materials, AIIM, Innovation Campus, University of Wollongong, Wollongong, NSW 2500, Australia

Email: cylee@uow.edu.au

# Experimental details

## 1. Synthesis details

Iron foil (thickness: 0.25 mm, 99.5%, Advent Research Materials), potassium hydroxide (90%, Sigma Aldrich), Nickel (II) sulfate hexahydrate (98%, Sigma Aldrich), ethanol (ChemSupply), acetone (ChemSupply). All materials and chemicals were used as received without further purifications. Mili-Q system deionized water was used to prepare all solutions.

Iron foil pre-treatment: Iron foils were cut into 1 × 1 $cm^2$ sheets with a neck of 0.5 × 1 $cm^2$, cleaned and ultrasonicated in acetone, ethanol, and distilled water, before being dried by purging under $N_2$ stream. Cleaned iron foil sheets were then annealed in air for 1 h at 400 $^oC$ and naturally cooled down, before further use (Fe-400).

Synthesis of Fe-400-nC: Electrochemical synthesis of iron oxyhydroxide nanosheets was performed on the annealed iron foil (Fe-400) as a working electrode, a platinum mesh as a counter electrode, and a double-frit Ag/AgCl (3 M NaCl) as a reference electrode, using a CH Instrument 650 potentiostat. Designated cyclic voltammetric (CV) cycles were applied to the annealed iron foils in 1 M KOH, unless otherwise stated. CVs were performed at 50 mV $s^{-1}$ over a potential window of 0 to -1.5 V vs. Ag/AgCl except for a study of potential effect from 0 to -1.0 V. Samples obtained using this procedure are denoted as follows: Fe-400-nC, where “400” corresponds to the heat treatment temperature in degrees Celcius and ‘‘n’’ corresponds to the number of CV cycles.

Synthesis of Fe-nC: Multiple CV method as described for Fe-400-nC samples, except the working electrode was a cleaned iron foil without thermal annealing.

Ni deposition: Ni was deposited onto the Fe-400-nC by electrodeposition in a solution of 0.01 M $NiSO_4$ and 0.2 M sodium citrate at -1.0 V vs. Ag/AgCl (3M NaCl) for either 1, 5, or 10 min.

## 2. Characterization.

A field-emission Scanning Electron Microscope (JEOL JSM-7500FA) was used to examine the surface morphology of the samples. X-ray diffraction (XRD) analysis was performed on PANalytical Empyrean XRD apparatus at a scan rate of $2^o$ $min^{-1}$. X-ray photoelectron spectra (XPS) were collected by illuminating the samples with a non-monochromatic X-ray source (Omnivac) using Al $K_\alpha$ (1486.6 eV) radiation and photoemission collected by an SES2002 analyser (Scienta). The working pressure in the analysis chamber during XPS measurements was typically ~4.5 x $10^{-9}$ mBar, with a base pressure of 9 x $10^{-10}$ mBar. XPS spectra were calibrated by referencing the primary C1s peak to 284.5 eV in accordance to the literature data.

## 3. Electrochemically active surface area (ECSA) study

The ECSA study of iron materials were estimated based on the electrochemical double-layer capacitance ($C_{\mathrm{dl}}$) examined by using CV method as the $C_{\mathrm{dl}}$ is proportional to the ECSA. The CV curves were taken in the non-faradaic current potential region (0 to 0.1 V vs. Ag/AgCl) shown in Fig. S4. The $C_{\mathrm{dl}}$ was measured by plotting the $\Delta j/2$ and scan rate, where $\Delta j = j_a - j_c$. $j_a$ and $j_c$ are the anodic and cathodic current densities at 0.05 V vs. Ag/AgCl. ECSA was calculated by the equation:

$$\mathrm{ECSA} = C_{\mathrm{dl}} / C_{\mathrm{s}},$$

where $C_s$ value was 0.040 mF $\mathrm{cm}^{-2}$, assuming that the electrode in KOH was atomically smooth.

## 4. Performance test and kinetic study

The performance tests were carried out using the same setup as described in the electrochemical synthesis part, employing 1.0 M KOH. The measured potentials vs. Ag/AgCl were converted to the reversible hydrogen electrode (RHE) scale according to the following Nernst equation: $E_{\mathrm{RHE}} = E_{\mathrm{Ag/AgCl}} + 0.0591 \times \mathrm{pH} + 0.1976$ V. The linear sweep voltammetry (LSV) measurements and kinetic studies were conducted at a 5 mV $\mathrm{s}^{-1}$. Tafel plot was obtained in 1.0 M KOH electrolyte at 5 mV $\mathrm{s}^{-1}$. Tafel equation, $\eta = a + b \log(j)$, in which “a” is the Tafel constant, “b” is the Tafel slope, and “j” is the current density, was employed to obtain linear fit and relevant Tafel slopes.

## 5. Thickness statistics for the nanosheets

The statistic value of nanosheet lateral sizes and thicknesses were obtained by the edges of the nanosheets marked in the SEM images. Some of the edges might be broadened because of the charging effect. Therefore, only sharp edges visible in the SEM images were included in the evaluation.

**Table S1**. Sizes of nanosheets grown under different conditions

| Samples | Growth conditions | Thickness(nm) | Diameter / lateral size (nm) |
|---|---|---|---|
| Fe-400-1C | -1.5 V - 0 V, 1 M KOH | 6±2 | 400±100 |
| Fe-400 -9C | -1.5 V - 0 V, 1 M KOH | 10±2 | 600±200 |
| Fe-400 -20C | -1.5 V - 0 V, 1 M KOH | 15±2 | 800±200 |
| Fe-9C | -1.5 V - 0 V, 1 M KOH | 20±2 | 250±50 |
| Fe-400 -9C | -1.0 V - 0V, 1 M KOH | N/A | N/A |
| Fe-400 -9C | -1.5 V - 0 V, 0.1 M KOH | 5±2 | 200±100 |
| Fe-400 -9C | -1.5 V - 0 V, 10 M KOH | 45±5 | 1500±500 |

**Table S2.** OER performance comparison of iron oxyhydroxides obtained by different methods

| Synthesis method | Require overpotential to reach j=10 mA $cm^{-2}$ | References |
|---|---|---|
| Chemical bath deposition method | > 0.55 V | [1] |
| Bath deposition method | 0.49-0.56 V | [2] |
| Solution method | 0.58 V | [3] |
| Hydrothermal method | 0.53 V | [4] |
| Thermal treatment & CV cycling | 0.43 V | This work |

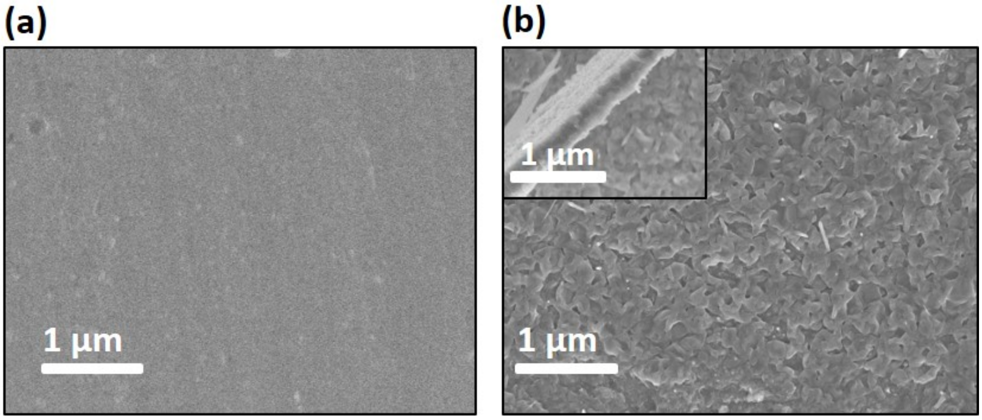

**Fig. S1**. SEM images of (a) clean bare Fe foil without further treatment and (b) Fe foil heat-treated at 400 °C for 1 h (Fe-400), with an inset showing cross sectional oxide layer of Fe-400.

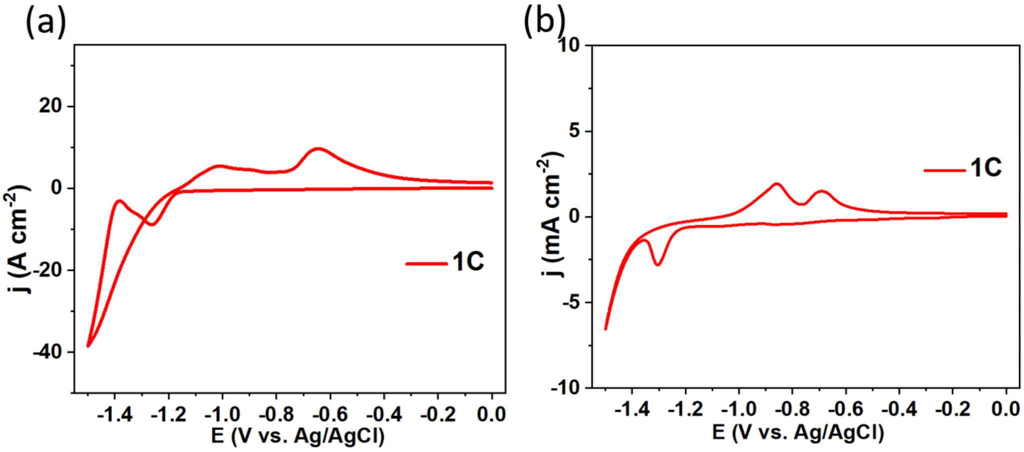

**Fig. S2**. CVs for the first cycles of annealed iron foil (a) and bare iron foil (b).

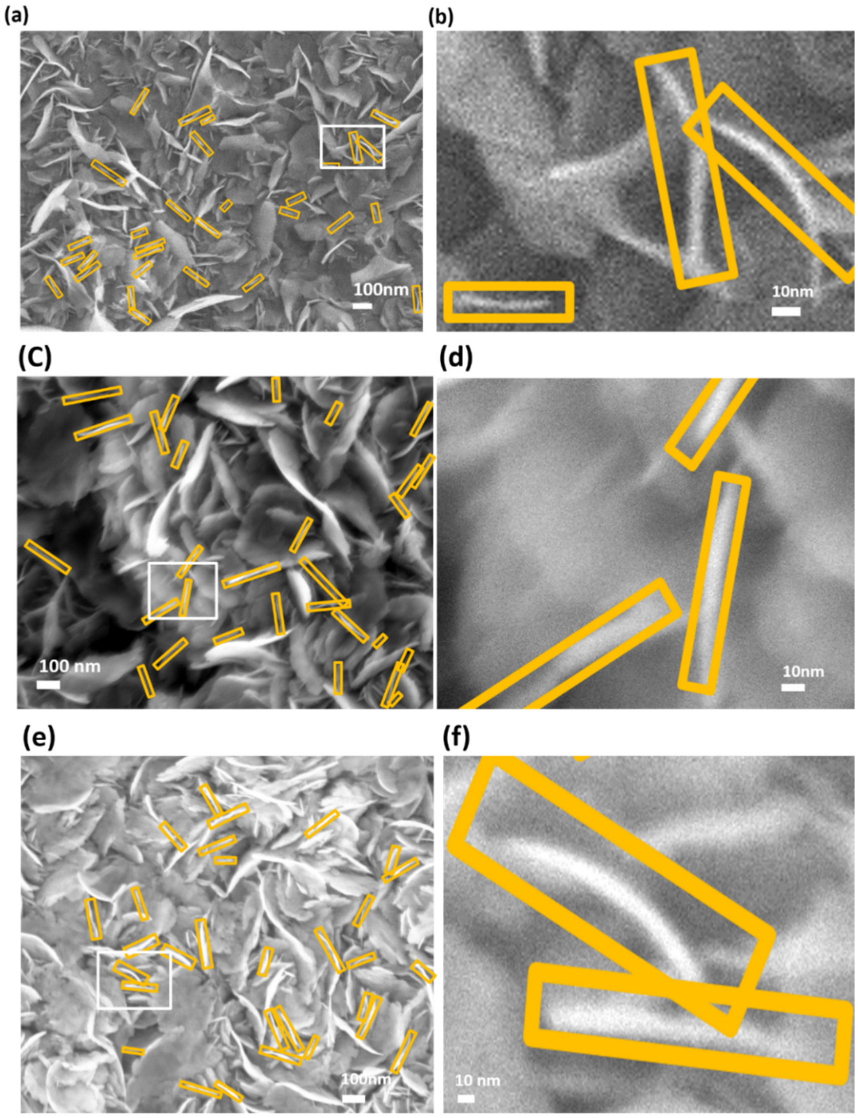

**Fig. S3**. SEM images of the Fe-400-1C (a) Fe-400-9C (c) and Fe-400-20C (e); (b), (d), and (f) are the enlarged image of the selected regions in (a) (c) and (e), respectively.

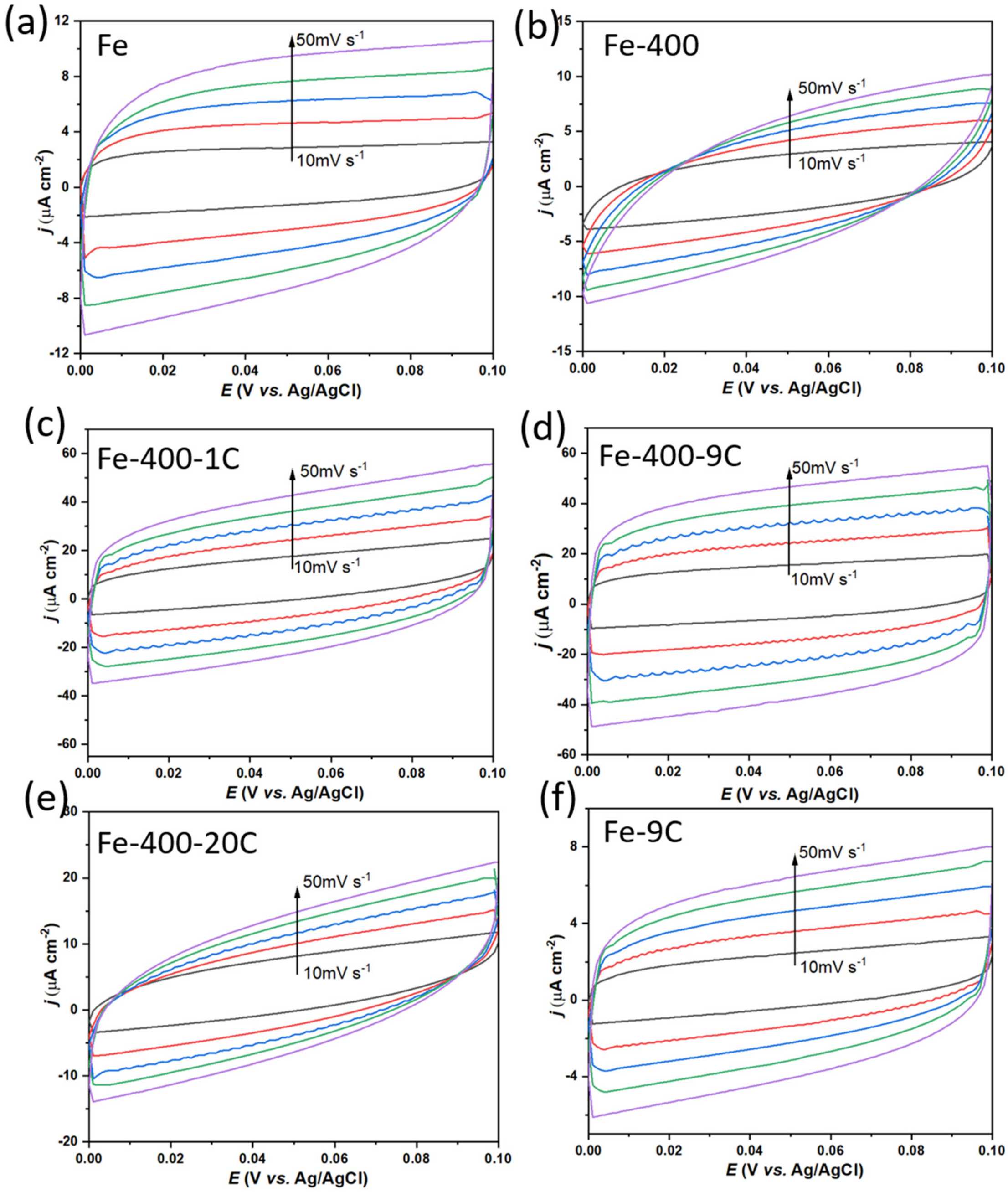

**Fig. S4.** CV curves of Fe (a), Fe-400 (b), Fe-400-1C (c), Fe-400-9C (d), Fe-400-20C (e), Fe-9C (f) for ECSA calculation performed at various scan rates in a 1.0 M KOH solution.

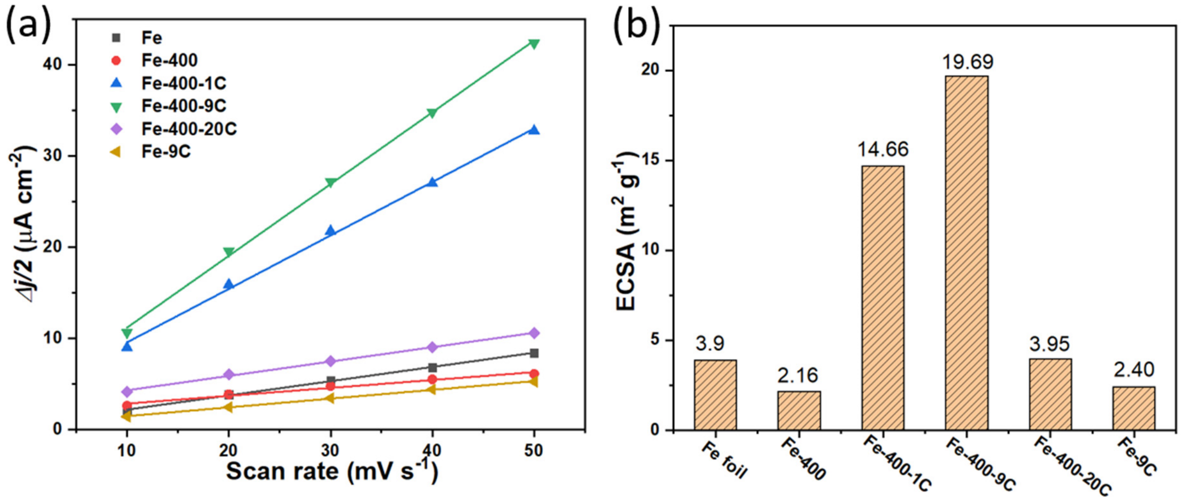

**Fig. S5.** The plots of (a) $\Delta j/2$ as a function of scan rate and (b) calculated ECSA for various iron-based samples. The ECSA was calculated by the equation: ECSA = $C_{dl}$ / $C_s$, where $C_s$ value was 0.040 mF cm$^{-2}$ and the $C_{dl}$ is the slope of $\Delta j/2$-Scan rate assuming that the electrode in KOH was atomically smooth.

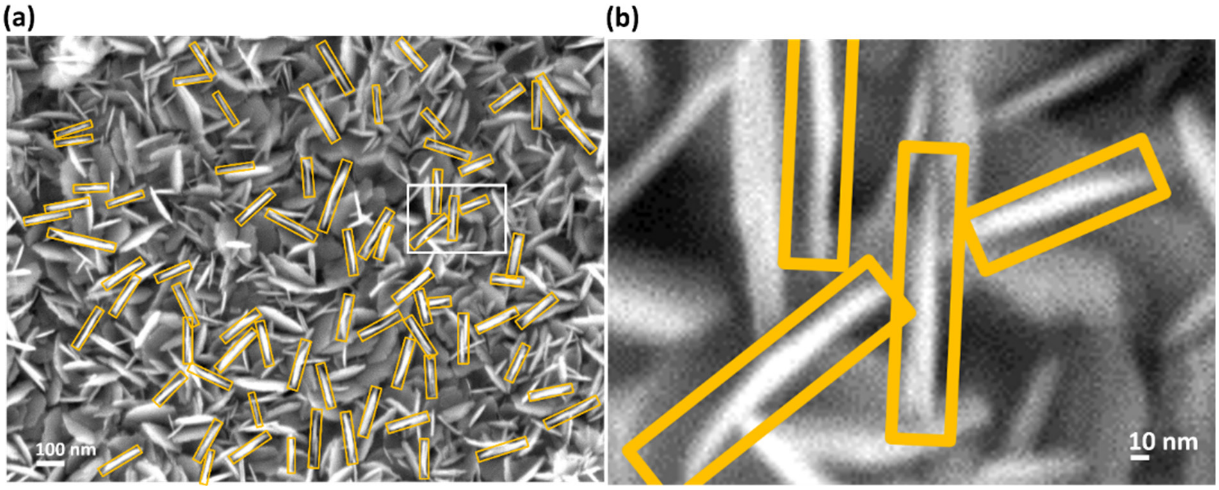

**Fig. S6**. SEM images of the Fe-9C (a) and the enlarged image of the selected region (b).

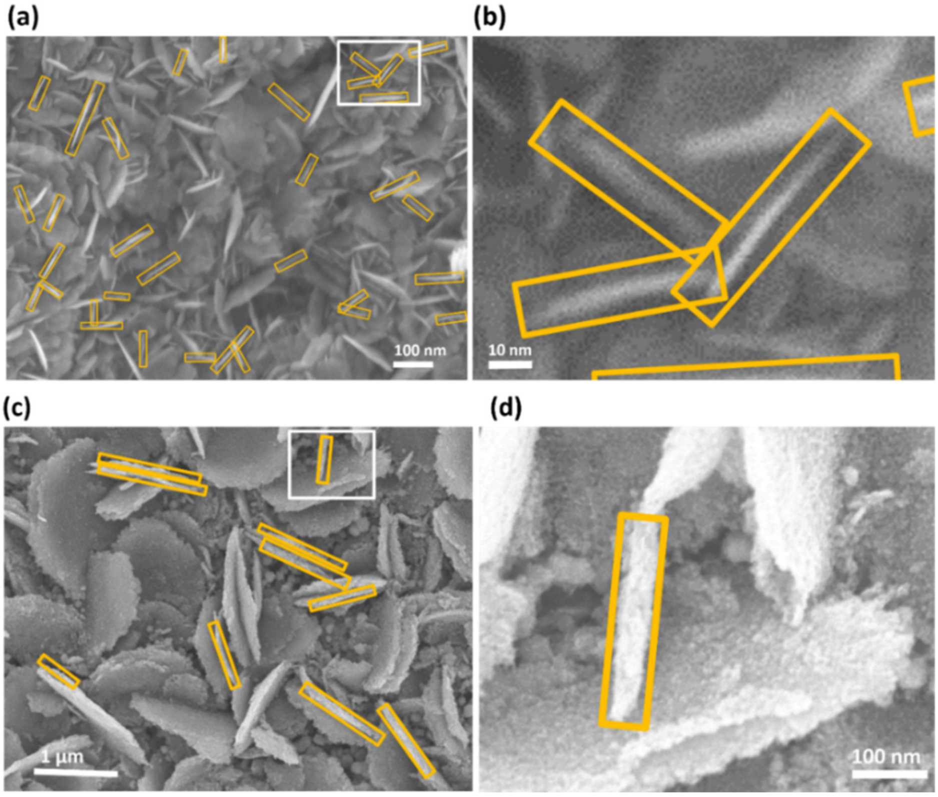

**Fig. S7**. SEM images of the Fe-400-9C grown in 0.1 M KOH (a) and 10 M KOH (c); (b) and (d) are the enlarged image of the selected regions in (a) and (c), respectively.

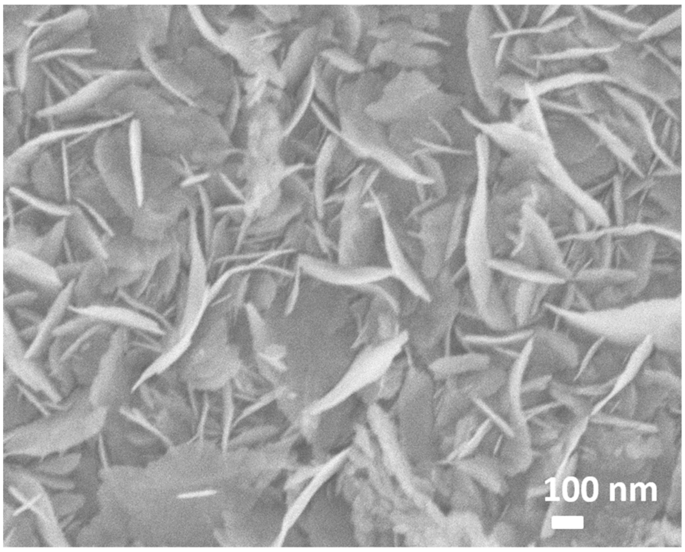

**Fig. S8.** SEM image of the Fe-400-9C after the stability test.

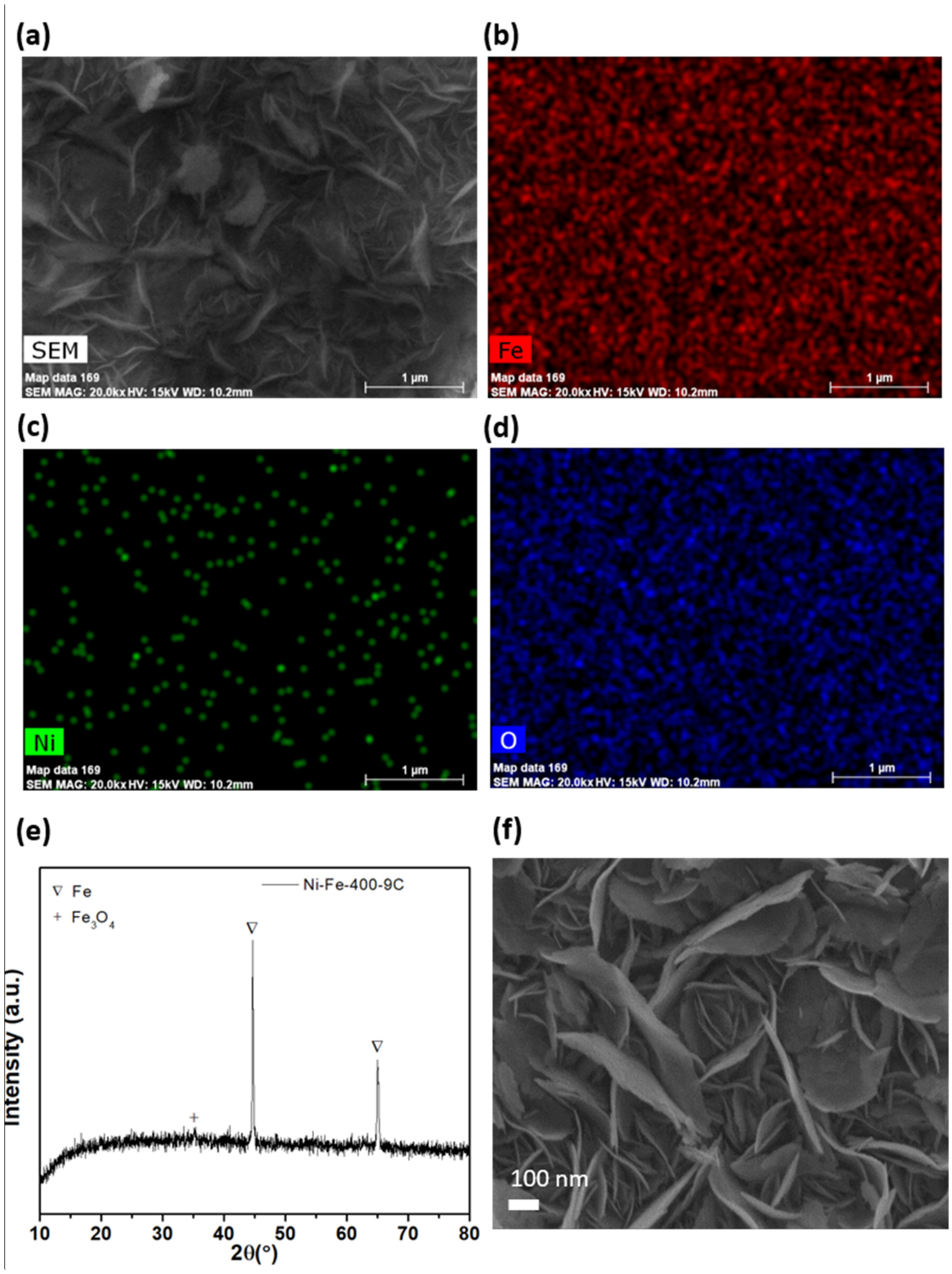

**Fig. S9**. Elemental mapping images of Ni-Fe-400-9C (a), (b), (c), (d); XRD pattern of Ni-Fe-400-9C (e) and SEM image of the Ni-Fe-400-9C after the 10 h stability test (f).

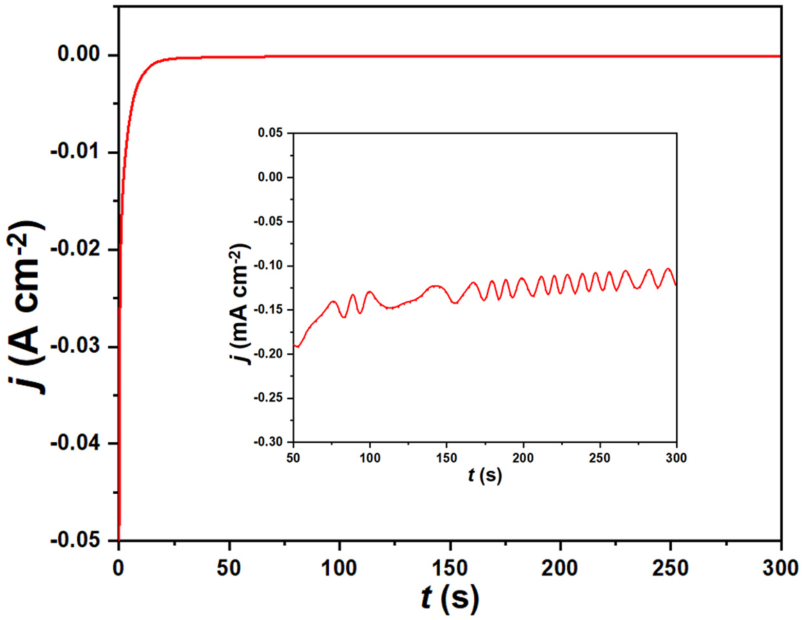

**Fig. S10** Current time profile of Ni loading of the Ni-Fe-400-9C sample, the inset is the enlarged curve from 50 to 300 s.

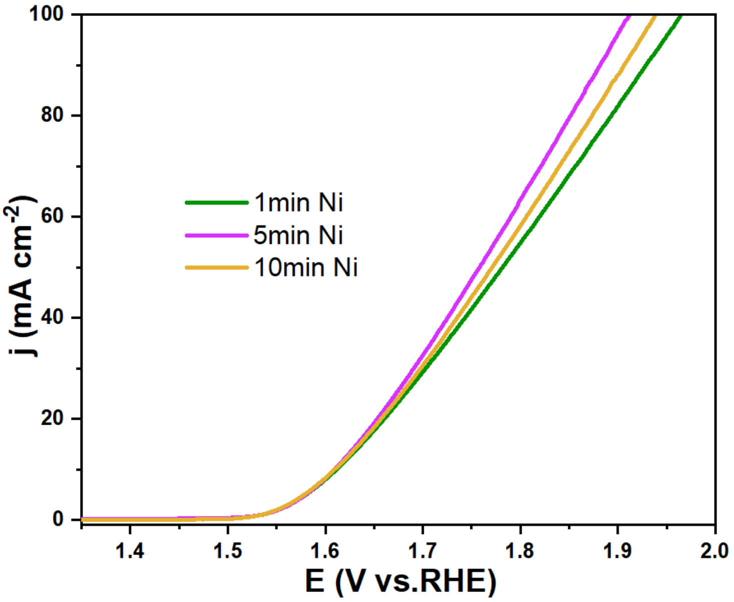

**Fig. S11**. Linear sweep voltammetry (LSV) of Ni-Fe-400-9C samples with different Ni loading time. All the measurements were conducted at a scan rate of 5 mV $s^{-1}$ in 1.0 M of KOH aqueous solutions.

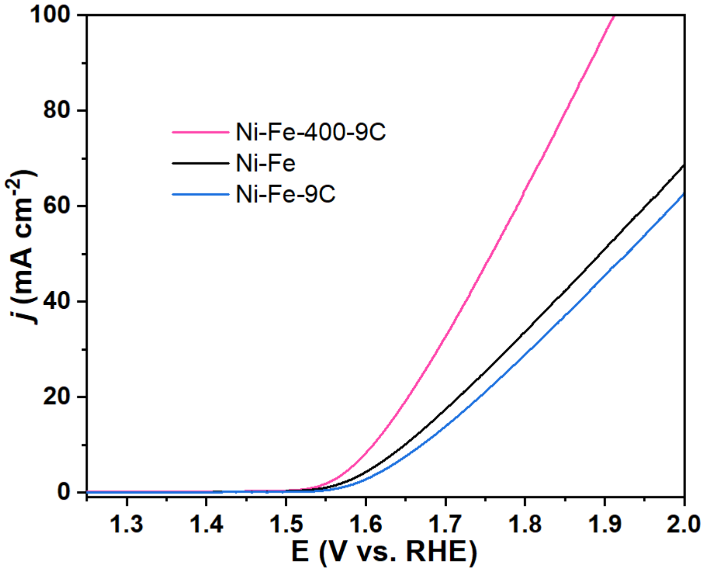

**Fig. S12** The OER performance comparison of Ni-Fe-400-9C, Ni-Fe, and Ni-Fe-9C

## References

[1] W. Luo, C. Jiang, Y. Li, S. A. Shevlin, X. Han, K. Qiu, Y. Cheng, Z. Guo, W. Huang and J. Tang, *J. Mater. Chem. A*, 2017, **5**, 2021-2028.

[2] W. D. Chemelewski, J. R. Rosenstock and C. B. Mullins, *J. Mater. Chem. A*, 2014, **2**, 14957-14962.

[3] D. Inohara, H. Maruyama, Y. Kakihara, H. Kurokawa and M. Nakayama, *ACS Omega*, 2018, **3**, 7840-7845.

[4] X. Zhang, L. An, J. Yin, P. Xi, Z. Zheng and Y. Du, *Sci. Rep.*, 2017, **7**, 43590.